A Spectral-Iteration Technique for Analyzing Scattering from Arbitrary Bodies, Part I: Cylindrical Scatterers with *E*-Wave Incidence

RAPHAEL KASTNER, STUDENT MEMBER, IEEE, AND RAJ MITTRA, FELLOW, IEEE

Abstract—**In the past, methods for solving electromagnetic scattering problems in the frequency domain have been developed largely for the low-frequency (moment method) and high-frequency (asymptotic techniques) regimes. The intermediate frequency range has been analyzed by combinations of these two approaches or by separation of variables, when possible. This paper is devoted to the development of an independent approach, viz., the "stacked spectral-iteration technique," which is capable of handling arbitrary scatterers with dimensions ranging from small to moderately large. The method takes advantage of the simplicity with which the planar-source planar-field relationships are expressed in the spectral domain. The boundary conditions or constitutive relationships, on the other hand, are expressed most simply in the spatial domain. Alternating between the two domains is carried out with the aid of the fast Fourier transform (FFT) algorithm. The spectral-iteration technique (SIT) was applied in the past to thin planar structures which allow the analysis to be carried out on a plane. The generalization of the two-dimensional formulation to arbitrary three-dimensional bodies can be accomplished by sampling the current distribution on the scatterer over a number of parallel planes, and using the simple spectral-domain interaction relationships between the planes. This new approach involves no matrix inversion and is capable of analyzing scatterers whose sizes far exceed those treatable by the moment method. In addition to being arbitrarily shaped, the scatterer may be conducting, dielectric, or lossy dielectric. Thus, the SIT provides an efficient approach to filling the much-needed gap between low- and high-frequency conventional techniques, e.g., the moment method (MoM) and the geometrical theory of diffraction (GTD), and to extending the range of applicability to dielectric scatterers, with or without loss. Though the concepts presented herein are applicable to arbitrary three-dimensional scatterers, the problem of arbitrary cylinders with *E*-polarized excitation is addressed in this paper, while the *H*-case is treated in an accompanying work. The three-dimensional case is to be reported in a future communication which treats the problem of scattering by a lossy inhomogeneous dielectric cylinder of finite length.**

I. INTRODUCTION

CONVENTIONAL approaches to solving electromagnetic radiation and scattering problems involve the use of either the matrix methods for low frequencies or asymptotic techniques, e.g., the ray method, for high frequencies. When the size of the scatterer is on the order of $(1\ \lambda)^3$ or more, the moment method (MoM), which results in a matrix formulation of the boundary-value problems, becomes severely limited because of prohibitive cost and computer storage requirements associated with the generation and inversion of a large matrix. The ray methods, which are based on the application of the geometrical theory or diffraction as introduced by Keller [1] and developed by many of his followers, are largely limited to frequencies above the resonance range and to scatterers that are perfect conductors.

Manuscript received June 26, 1982; revised September 20, 1982. This work was supported in part by the Office of Naval Research under Contract N00014-81-K-0245 and in part by the Joint Services Electronics Program under Contract N00014-79-C-0424.

R. Kastner was with the Electromagnetics Laboratory, Electrical Engineering Department, University of Illinois, Urbana, IL. He is now with RAFAEL, Haifa, Israel.

R. Mittra is with the Electromagnetics Laboratory, Electrical Engineering Department, University of Illinois, 1406 West Green Street, Urbana, IL 61801.

For these reasons, the need for a general approach to solving scattering problems in the intermediate or resonance frequency range, and for arbitrary scatterers including inhomogeneous dielectric bodies, has long been recognized. Unfortunately, except for limited cases, it is difficult to bridge the gap between the two frequency ranges by combining the MoM with the geometrical theory of diffraction (GTD) in a straightforward manner, though this has proven useful for a class of geometries [2], [3]. The purpose of this paper is to present a new scheme, hereafter referred to as the stacked two-dimensional spectral-iteration technique (SIT), which is based on the use of the Fourier transform technique and which exhibits good potential for attacking the problem of scattering from arbitrary scatterers. The method takes advantage of the simplicity with which the relationship between planar sources and fields is expressed in the spectral domain. When the field is evaluated on a plane next to a thin planar current distribution lying say in the x-y plane, the integral relating the current to the field is a convolution between the current and the Green's function. Hence, the relationship between the spectral current and the spectral field involves an algebraic multiplication of the current by the spectral Green's dyad. That is, in the spectral domain, we write

$$\tilde{\mathbf{E}}(k_x, k_y) = \tilde{\mathbf{G}}_e \cdot \tilde{\mathbf{J}}(k_x, k_y). \tag{1}$$

The quantities k_x and k_y in (1) are the Fourier transform variables introduced as follows:

$$\tilde{\mathbf{E}}(k_x, k_y) = \int_{-\infty}^{\infty} \mathbf{E}(x, y, 0) e^{j(k_x x + k_y y)}\, dx\, dy. \tag{2}$$

One very efficient approach for solving the class of planar problems is the SIT [4]-[6] which involves no matrix inversion. This technique can be extended to include dielectric planar bodies (see Section II). It then serves as a building block for the arbitrary scattering problem, specialized at this stage to the problem of scattering from arbitrary cylinders that can be formulated by modeling the current distribution on the cylinder by a set of parallel, linear current distributions (see Fig. 1). This stacked modeling makes it possible to extend the capabilities of the spectral-domain approach to arbitrarily shaped, perfectly conducting, to (lossy) dielectric cylindrical scatterers. The stacked SIT repeatedly applies the Fourier transform algorithm to the set of linear distributions and generates the solution to the original two-dimensional problem in an iterative manner.

A conceptually similar algorithm was formulated by Bojarski [7] for the three-dimensional case and was based upon the use of a three-dimensional k-space as the Fourier transform domain. In reality, however, the spectral representation of fields contains no more than two independent variables, the third one being related to them via the dispersion relationship which describes a spherical two-dimensional shell in the three-dimensional k-space. Hence, simultaneously processing the entire three-dimensional set of unknowns is not economical. A unique feature of the stacked SIT is that it reuses the storage allocated for a

0018-926X/83/0500-0499$01.00

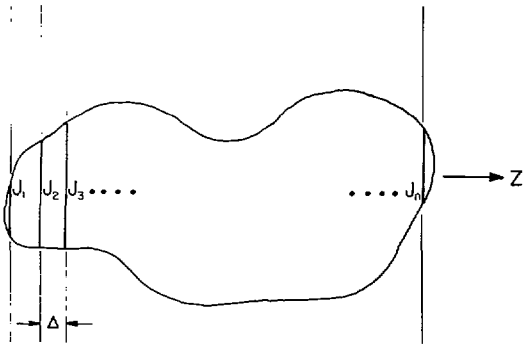

Fig. 1. Planar current samples on the cross section of a cylinder.

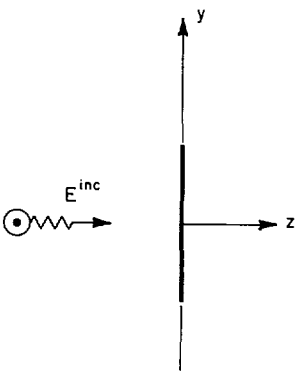

Fig. 2. Isolated strip.

single plane (or a single line, for the cylindrical case) over and over again as it performs the computation at other planes. This eases the burden on storage requirements considerably (see Section VI).

Computational efficiency and low storage requirements make the spectral-iteration method capable of handling a rather large number of unknowns, on the order of 2000 or more, far beyond the reach of the matrix methods. This feature of the spectral technique enables one to attack moderate-to-large size scatterers which were previously considered to be unmanageably large and beyond the scope of the moment method and other available techniques.

The SIT thus provides an alternative to moment methods, high-frequency asymptotic techniques, and their combinations, especially in the intermediate frequency range where conventional methods are very limited in scope.

The extension of the procedure developed for planar conducting [4] to planar dielectric structures is discussed in Section II. This forms the building block for the stacked SIT for arbitrary cylinders given in Section III. Results for conducting and dielectric cylinders are described in Sections IV and V, respectively, and a quantitative comparison to other methods is given in Section VI.

A similar procedure has proved to be useful for cylinders with H-wave illumination and is described in an accompanying work [8]. The more general three-dimensional dielectric case will be reported in an upcoming paper.

II. THE BUILDING BLOCK FOR SIT: THE SINGLE STRIP

The SIT for general scatterers may be viewed as a generalization of the two-dimensional scheme [4] for the single strip. (See Fig. 2.) This scheme is now reformulated to accommodate dielectric strips as well. The conducting strip may be regarded as a special case with $\epsilon_r \to 1 - j\infty$. To this end, we use polarization current

$$J = j\omega\epsilon_0(\epsilon_r - 1)(E + E^{\text{inc}}) \tag{3}$$

as the current source for the free-space wave equation.

Equation (3) serves as the "constitutive relationship" which plays an analogous role to the boundary condition in the conducting case. Equation (3) is algebraic in the spatial domain, whereas (1) is algebraic in the spectral domain. An iterative procedure for solving this system of equations alternates between the two domains by use of the FFT algorithm. It is depicted graphically in Fig. 3 and a step-by-step outline follows.

1) Begin with an initial guess $\mathbf{J}^{(0)}$.
2) Take the two-dimensional transform of $\mathbf{J}^{(0)}$ on the planar structure to obtain $\tilde{\mathbf{J}}^{(0)}$.

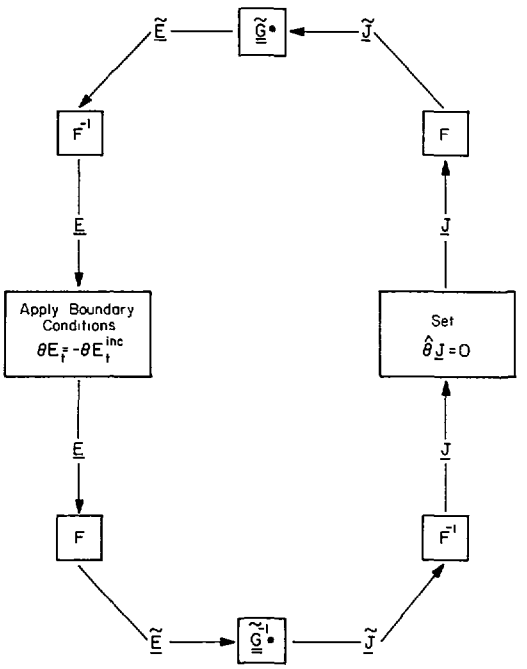

Fig. 3. Iteration scheme for conducting planar scatterers.

3) Multiply $\tilde{\mathbf{J}}^{(0)}$ by $\tilde{G} = j\omega\mu/2\sqrt{k_0^2 - k_y^2}$.
4) Evaluate $\mathbf{E}^{(0)} = F^{-1}[\tilde{G}\cdot\tilde{\mathbf{J}}^{(0)}]$, the approximation to the scattered electric field $\mathbf{E}$. The accuracy of the solution can be conveniently checked at this point by verifying the satisfaction of the constitutive relationshp (3) within the scatterer. This is an important feature of the method.
5) Update $\mathbf{E}$ by applying the constitutive relationship: Replace $\mathbf{E}_t$ within the body, $\theta\mathbf{E}_t$ (θ equals truncation operator; it is defined by $\theta = 1$ on scatterer and $\theta = 0$ outside scatterer) by $\theta(-\mathbf{E}_t^{\text{inc}}) + (\mathbf{J}/j\omega\epsilon_0(\epsilon_1 - 1))$, leaving the field outside the body unchanged.
6) Take the Fourier transform of the updated field obtained in step 5.
7) Multiply the result obtained in Step 6 by $\tilde{G}^{-1}$. The result thus obtained is $\tilde{\mathbf{J}}^{(1)}$, which is the transform of the first iteration of the current.
8) Take the inverse Fourier transform of $\tilde{\mathbf{J}}^{(1)}$ obtained in step 7 to get the surface current on the scatterer. In other words, perform the operation $\theta(F^{-1}[\tilde{\mathbf{J}}^{(1)}])$. For an exact solution, the truncation is redundant, since $\mathbf{J} = \theta\mathbf{J}$, and, hence, $\theta(F^{-1}[F[\theta\mathbf{J}]]) = \theta\theta\mathbf{J} = \mathbf{J}$. However, the Fourier inversion of the nth approximate solution $\tilde{\mathbf{J}}^{(n)}$ will not give rise to a current distribution that is nonzero except on S.

This step provides a test for the accuracy and for the convergence of the approximate solution by comparing the approximate $\mathbf{J}^{(0)}$ with $\theta(F^{-1}[\tilde{\mathbf{J}}^{(1)}])$.

9) Repeat as necessary using the improved $\mathbf{J}^{(1)}$ from step 8 in step 1 above to generate the next higher order approximation $\mathbf{J}^{(2)}$ and continue in this manner until convergence has been attained.

Recall that the conducting strip scheme of [4] may be viewed as a special case of the above procedure with $\epsilon_r \to 1 - j\infty$. Step 5 then implies imposing the boundary condition $E = -E^{\text{inc}}$ within the body. Results of the above procedure for conducting strips are given in [4].

III. ARBITRARY CYLINDERS WITH E-MODE EXCITATION

The approach to handling the general-shaped cylindrical scatterer is to sample the induced current on it by a collection of n linear distributions in free space, as shown in Fig. 1. For this case, $\partial/\partial x \equiv 0$, or $k_x \equiv 0$, and $\mathbf{J} = J_x\tilde{x}, \mathbf{E} = E_x\tilde{x}$. The single-strip scheme of Section II can be used to solve the original problem which is now reduced to that of determining the linear currents. For a perfectly conducting scatterer, these currents are confined to the edges of the cross-sectional lines dissecting the body. For a dielectric scatterer, however, the currents flow in the interior of the body as well.

The strategy for attacking the reduced problem is as follows. We employ the basic iterative scheme outlined in Section II for linear structures to update the individual linear distributions in a sequential manner, starting with the first line and ending up at the last one. We update the currents in one particular line by applying a single iteration cycle as in Fig. 3 while regarding the distributions in the other lines as temporarily known from previous operations. This sequential processing facilitates the reuse of the same storage area for all the linear currents. This significantly reduces the burden on the computer memory and cost as compared to the direct solution of a two-dimensional problem carried out in one fell swoop. The iteration process encompassing all the lines is repeated as many times as necessary until convergence of the entire current distribution is achieved.

The enforcement of the boundary condition on the scatterer requires the computation of the scattered field produced by all of the linear induced current distributions. This is done as follows.

Assume that the line at which the scattered field is being evaluated is p_+, immediately to the right of the current slice J_p (Fig. 4). It is evident that the sources J_1 through J_p lie to the left of this line, while J_{p+1} through J_n are on the right of p_+. Consider first the left sources, the fields from which propagate to the right ($+z$) direction; hence, their spectrum has the z-dependence exp $[-jz\sqrt{k_0^2 - k_y^2}]$. Let us denote this part of the field by $E_{p+}^{(-)}$ where the superscript indicates that the currents generating this field are on the left of the line of evaluation:

$$\tilde{E}_{p+}^{(-)} = \tilde{G} \cdot \Delta \sum_{i=1}^{p} \tilde{J}_i e^{-j\sqrt{k_0^2 - k_y^2}\cdot(p-i)\Delta} \tag{4}$$

where $\tilde{G}$ is the transform of the Green's function given for the E-case by

$$\tilde{G} = j\omega\mu \frac{j}{2\sqrt{k_0^2 - k_y^2}}. \tag{5}$$

Similarly $E_{p+}^{(+)}$, the aggregate of fields radiated by the sources on the right of the line p_+, may be written in the transform domain as

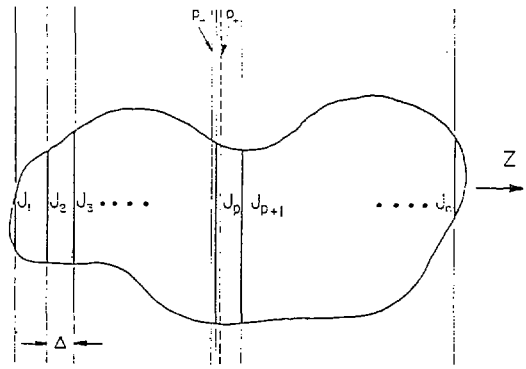

Fig. 4. Sliced scatterer with the lines p_- and p_+ shown immediately to the left and right of J_p, respectively.

$$\tilde{E}_{p+}^{(+)} = \tilde{G} \cdot \Delta \sum_{i=p+1}^{n} \tilde{J}_i e^{j\sqrt{k_0^2 - k_y^2}\cdot(p-i)\Delta}. \tag{6}$$

The total transformed field at the line p_+ is then a superposition of $E_{p+}^{(-)}$ and $E_{p+}^{(+)}$.

The separate bookkeeping of the two components $E^{(-)}$ and $E^{(+)}$ is necessary to facilitate transformation of the field between lines so that the sequential processing can be done. Suppose for example that the field at the line $(p+1)_-$ is desired. Since the region between the lines p_+ and $(p+1)_-$ is free space the following equations are valid:

$$\tilde{E}_{(p+1)_-}^{(-)} = \tilde{E}_{p+}^{(-)} e^{-j\sqrt{k_0^2 - k_y^2}\Delta} \tag{7a}$$

$$\tilde{E}_{(p+1)_-}^{(+)} = \tilde{E}_{p+}^{(+)} e^{+j\sqrt{k_0^2 - k_y^2}\Delta} \tag{7b}$$

Next, in order to transform the field from the line $(p+1)_-$ to $(p+1)_+$, we note that these two adjacent lines are located on each side of the thin current distribution J_{p+1}. Consequently we subtract the contribution of J_p from $E^{(-)}$ and add this contribution to $E^{(+)}$. This gives

$$\tilde{E}_{(p+1)_+}^{(-)} = \tilde{E}_{(p+1)_-}^{(-)} + \tilde{G} \cdot \tilde{J}_{(p+1)}\Delta \tag{8a}$$

$$\tilde{E}_{(p+1)_+}^{(+)} = \tilde{E}_{(p+1)_-}^{(+)} - \tilde{G} \cdot \tilde{J}_{(p+1)}\Delta. \tag{8b}$$

The above equations are consistent with the requirement that the total field be continuous across the plane.

A typical updating cycle at the line p is done similarly to that for the single strip case, by computing the total scattered field by the superposition of $E^{(-)}$ and $E^{(+)}$. One can now take the inverse transform of this scattered field due to the induced sources and enforce the boundary condition which may be expressed as

$$\text{(i)}\ E_{p+}^{(-)} + E_{p+}^{(+)} = -E_{\text{inc}}, \quad \text{inside a perfectly conducting body} \tag{9a}$$

$$\text{(ii)}\ E_{p+}^{(-)} + E_{p+}^{(+)} = -E_{\text{inc}}, \quad \text{inside a lossy dielectric scatterer described by a complex, relative permittivity } \epsilon_r. \tag{9b}$$
$$+ \frac{J(x,y)}{j\omega\epsilon_0[\epsilon_r(x,y) - 1]}$$

We replace the scattered field values inside the body with those dictated by the boundary condition while leaving the scattered

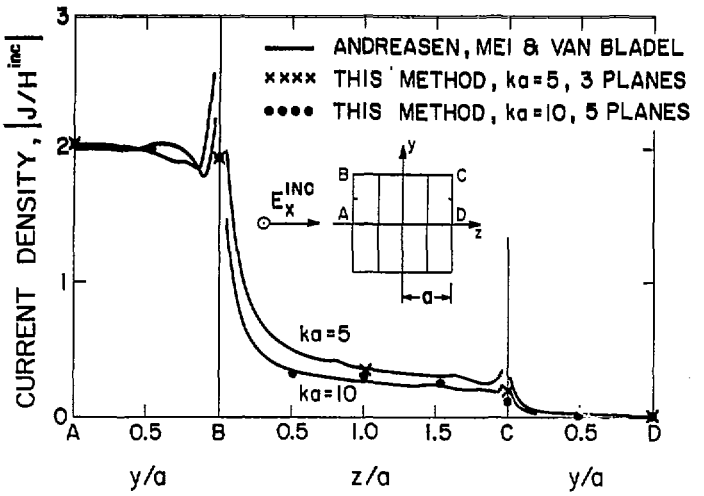

Fig. 5. Current distribution on a square cylinder illuminated by an E-mode incident field.

field outside the body unchanged. A Fourier transform of the updated total field is then taken. We then note that $\tilde{E}_{p+}^{(+)}$ is the field produced by currents located to the right of p_+. These currents are assumed to be temporarily known, hence, $\tilde{E}_{p+}^{(+)}$ is not changed during this cycle. $\tilde{E}_{p+}^{(-)}$, on the other hand, depends on J_1 through J_p and is updated. This is accomplished as follows:

$$\tilde{E}_{p+}^{(-)} = \tilde{E}_{p+} - \tilde{E}_{p+}^{(+)}. \tag{10}$$

The current J_p itself is next updated using a relationship analogous to step 7 in the single strip case above:

$$\tilde{J}_p = \tilde{G}^{-1} \cdot (\tilde{E}_{p+}^{(-)} - \tilde{E}_{p-}^{(-)})\Delta^{-1}. \tag{11}$$

$\tilde{E}_{p-}^{(-)}$ in the above equation is the contribution of the currents J_1 through J_{p-1} which are also assumed to be temporarily known from the previous cycle.

The process of updating the current on line p is now complete. We transform the updated field to line $p + 1$ by using (7a) and (8a), and repeat the entire process for that line. We then continue in this manner until the entire body has been scanned once. This constitutes one iteration step. The entire scanning process is then repeated until convergence is achieved and the results of the boundary condition test have been found to be satisfactory.

Certain numerical considerations sometimes require a slight modification of the above iteration procedure. First, it is often necessary to use a relaxation factor, which is used to form a weighted average of the new and old currents in order to update the induced current at a plane during iteration. Second, certain smoothing and filtering functions are often needed when truncating the scattered E-field and enforcing the boundary condition. Other numerical considerations include the choice of sampling rate, smoothing and data handling requirements; a discussion of these topics may be found in [9].

IV. RESULTS FOR CONDUCTING CYLINDERS

To illustrate the application of the spectral-iteration procedure to nonplanar solid scatterers, the case of a square conducting cylinder with E-mode excitation as shown in the inset of Fig. 5 is first considered. The edge-on incidence has been investigated for this geometry because it is more difficult to handle using ray methods. The sampling interval chosen is $\Delta = 0.8\ \lambda$ which is rather large. This large sampling interval has the effect of smoothing the current at the corners where, according to the moment method calculation of Mei and Van Bladel [10], it exhibits a singular behavior. Except for this expected smoothing, the comparison with the moment method results appears to be quite favorable. Incidentally, the singular behavior could also be reproduced using the iteration technique if the sampling interval is reduced to $\lambda/20$, as in the case of an isolated plate.

It is found that for this example convergence is achieved even with an initial guess of $J \equiv 0$. However, a physical optics approximation for the initial current renders the convergence much more rapid as shown in Fig. 6. A total of about 15 iterations were needed to bring the relative error in the field at each plane inside the body to within ten percent for a zero initial guess, while three or four iterations were sufficient when an initial physical optics guess was used. The updated current at each cycle of the iteration was averaged with the previous approximation by a weighting determined by a "relaxation factor" of 0.5. A higher weight for the updated version results in less uniform and slower convergence.

An even lower relaxation factor is needed when the amount of data is increased, especially if the initial guess is poor, as in Fig. 7, where the same problem was analyzed with $\Delta = 0.265\ \lambda$. Again, a total of 10 to 15 iterations are needed for a zero initial guess. Interestingly, as seen from Figs. 6 and 7, even when the initial guess is poor, the approximation improves already during the first iteration as the body is scanned away from the first plane. Most of the later iterations are needed to improve the current on the first few planes.

Another E-mode case, a square cylinder with an incident field at 45° to the cylinder face, is shown in Fig. 8. The slices are again arranged along the direction of propagation; this leads to faster convergence, although deviation from this direction is possible. The resultant current distribution is shown in Fig. 9, and again, comparison with the results in [11] is very good.

The manner in which we have sampled the scatterer requires the body to conform to a rectangular grid. An approximation of the shape is sometimes needed, as in Fig. 10, where the original body is an elliptical cylinder. When this is done, the results for the current distribution and the far scattered field in the forward direction are as shown in Figs. 11 and 12, respectively. Agreement with those in [11] is very good.

The above examples of small bodies have been investigated

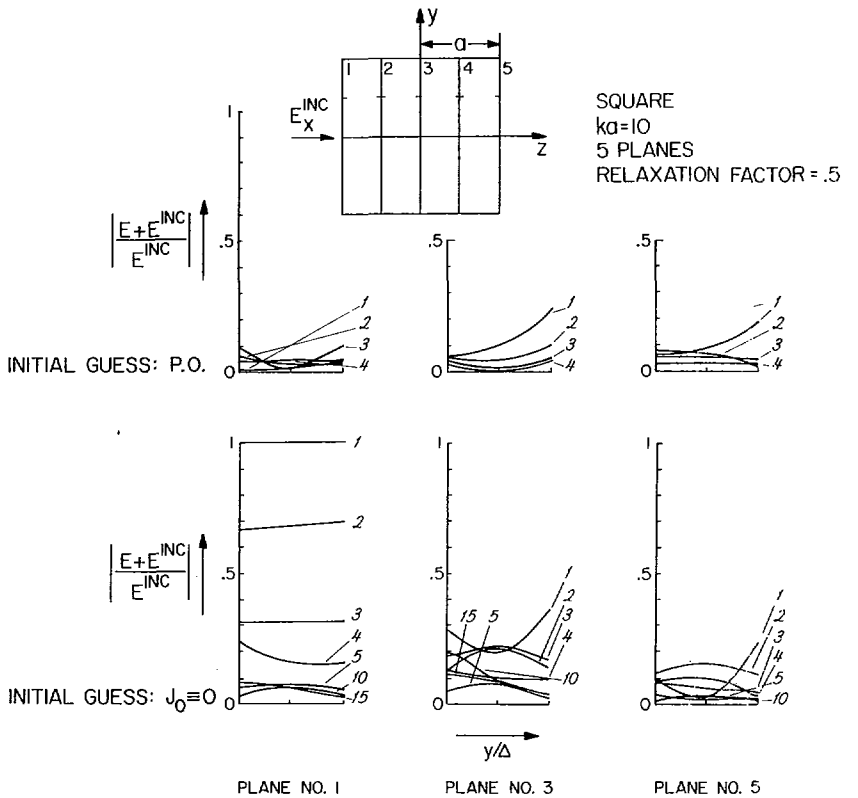

Fig. 6. Convergence of the solution of Fig. 5.

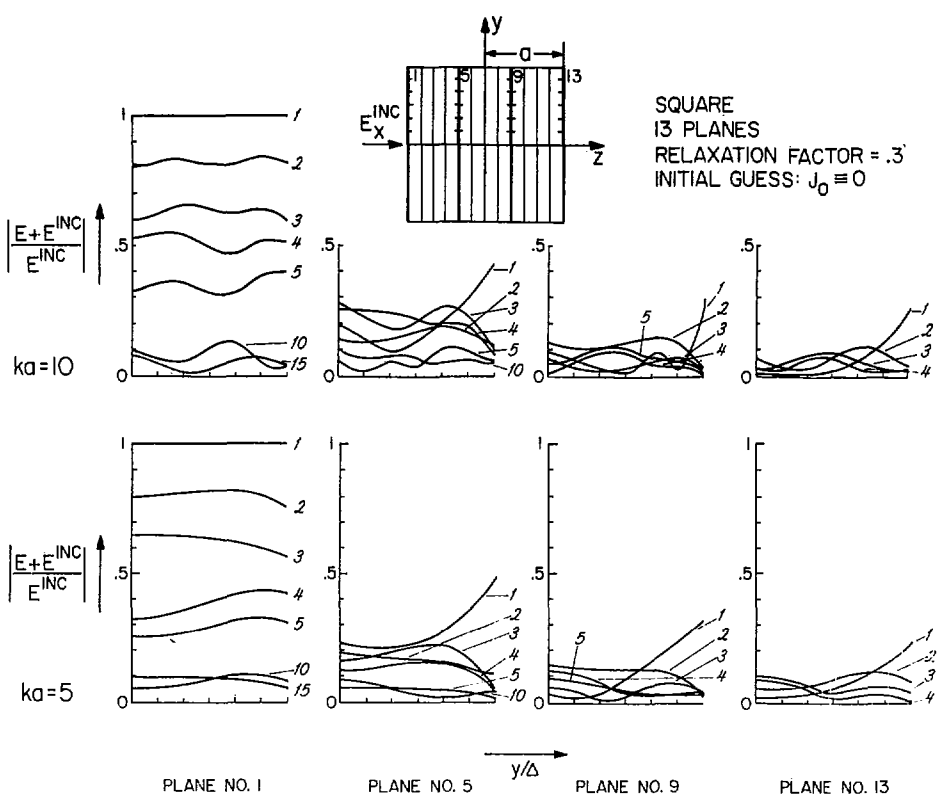

Fig. 7. Convergence of the solution for the sturcture of Fig. 5 obtained with 13 planes.

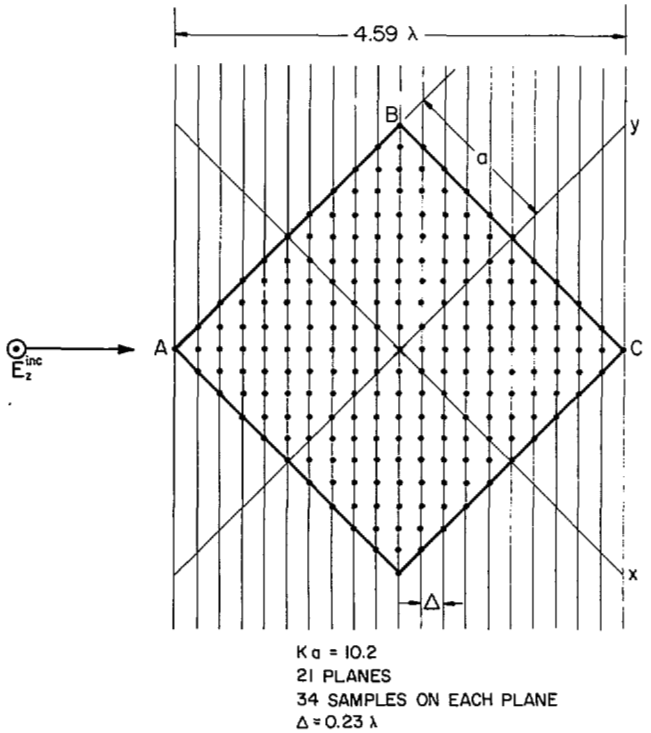

Fig. 8. Sampling grid for a square cylinder illuminated by an E-mode field incident at 45° to the cylinder faces.

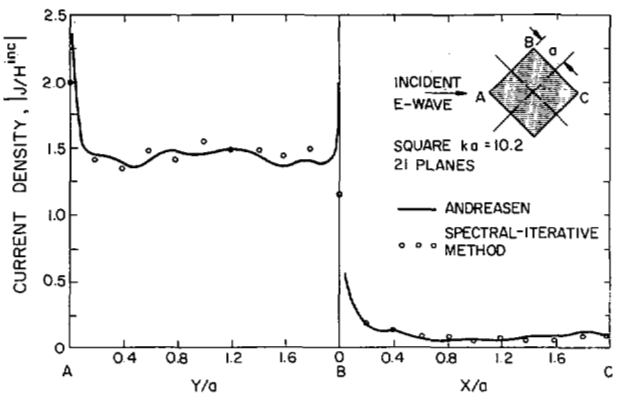

Fig. 9. Current distribution for the structure of Fig. 8.

so that this method can be compared to numerical results found in the literature. However, the capabilities of this method extend well beyond those of moment methods, especially if a low sampling rate is used. Applying the sampling rate of Fig. 5 to a 64-line body, one can treat a 50 λ scatterer as shown in Fig. 13, which falls far beyond the scope of the conventional numerical techniques. The validity of the solution can be asserted by the compliance with the boundary conditions. This case does not converge as easily as those for the smaller bodies; a relaxation factor of 0.2 was used to arrive at these results.

V. RESULTS FOR DIELECTRIC ARBITRARY CYLINDERS

The E-mode case for dielectric cylinders is very similar to that for the conducting case. The difference lies in the application of the constitutive relationship:

$$E = -E^{inc} + \frac{J}{j\omega\epsilon_0(\epsilon_r - 1)} \tag{12}$$

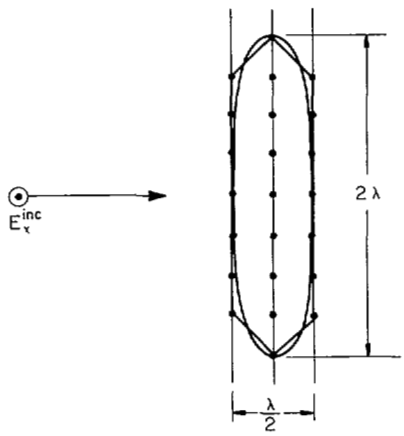

Fig. 10. Approximation to an elliptical cylinder.

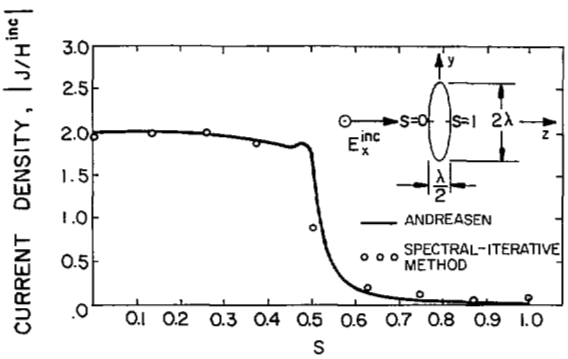

Fig. 11. Current distribution for the elliptical cylinder shown in Fig. 10.

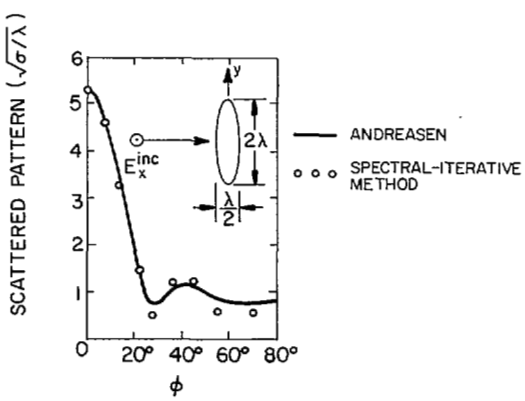

Fig. 12. Far scattered field from the elliptical cylinder shown in Fig. 10. ϕ is measured from the z-axis.

Fig. 13. Current distribution on a 50.1 λ by 3.2 λ cylinder illuminated by an E-mode incident field. Axes are arranged as in Fig. 5.

in lieu of the boundary condition $\bar{E}_{tot} = 0$ inside the scatterer when it is perfectly conducting. The dielectric case also differs from the conducting one by the fact that the polarization current is distributed throughout the volume rather than on the surface only (it is concentrated in regions closer to the surface for larger ϵ_r).

The fact that the solution for dielectric bodies requires the same data-handling capacity as the one for conducting bodies is one feature of this method that makes another difference between it and moment methods. For moment methods, the conducting problem is formulated on a surface, while the dielectric problem typically involves computations over the volume of the body (particularly for inhomogeneous dielectrics), making the dielectric problem more complicated by an order of magnitude. Since the spectral method naturally treats a scatterer in terms of a volume type of description, the advantages gained over the moment methods are even more significant for dielectric bodies.

Published examples for dielectric scatterers of reasonable size are even more scarce than for metallic ones. Three such examples are shown in Figs. 14-16.

Fig. 14 shows the result of applying the spectral-iteration method to a thin dielectric strip of 2.5 λ width compared to those of Richmond [12].

The case of an inhomogeneous strip is shown in Fig. 15 and compared to that in [12]. The ϵ_r variation is linear; the highest point is $\epsilon_r = 4$ at the center, and the lowest points are $\epsilon_r = 1$ at the edges.

A multisliced case is shown in Fig. 16. The thin strip, subject to E-mode illumination, has been sliced by lines along the direction of propagation of the incident field. The inverval between planes is $\Delta = \lambda/40$. The thin body occupies only one point at each plane according to this model. The results shown in Fig. 16 are in very good agreement with those published by Richmond [12].

Dielectric cylinders ranging in size to 3.16 λ by 50.1 λ have been analyzed. To the best of the authors' knowledge, no other existing method is capable of analyzing dielectric structures of this size. As in the large conducting case (Fig. 13), a small relaxation factor was chosen to facilitate smooth convergence. More dielectric examples, pertaining to living issues, will be presented in an upcoming paper.

VI. A COMPARISON BETWEEN THE SPECTRAL ITERATIVE TECHNIQUE, THE MOMENT METHOD, ASYMPTOTIC TECHNIQUES, AND BOJARSKI'S THREE-DIMENSIONAL K-SPACE METHOD

The stacked two-dimensional SIT has been applied to intermediate-sized scatterers which cannot be treated by moment methods with present-day computers. Besides being more versatile, the SIT avoids the complexity of some hybrid techniques based on a combination of moment method and asymptotic techniques. The spectral-iteration method is capable of handling scatterers whose sizes range from small to fairly large. It can also be used to analyze dielectric scatterers where conventional methods are even more limited.

Comparison to Bojarski's Method

Bojarski's method [7], which was the first one to consider FFT-based transform-domain techniques to solve scattering problems, was formulated in the entire three-dimensional K-

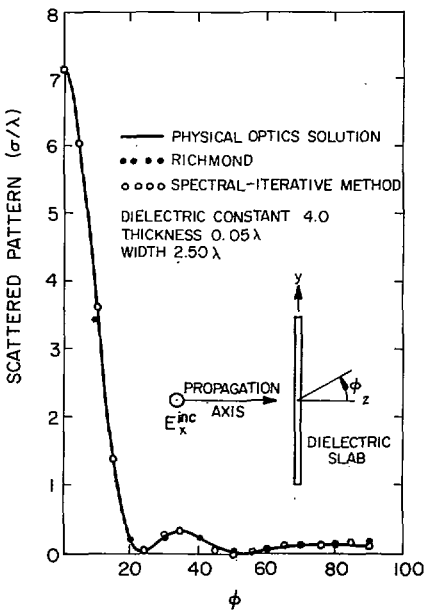

Fig. 14. A homogeneous thin dielectric strip.

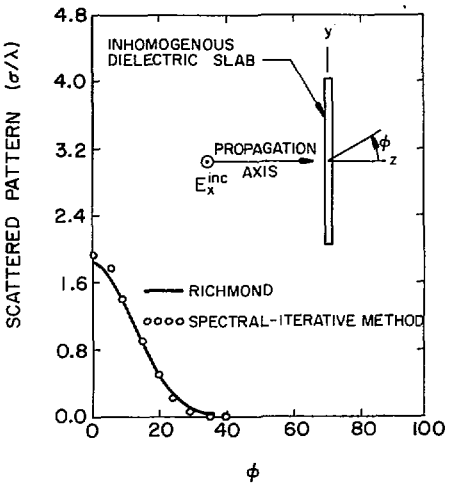

Fig. 15. An inhomogeneous thin dielectric strip: ϵ_r varies linearly from four at the center to one at the edges.

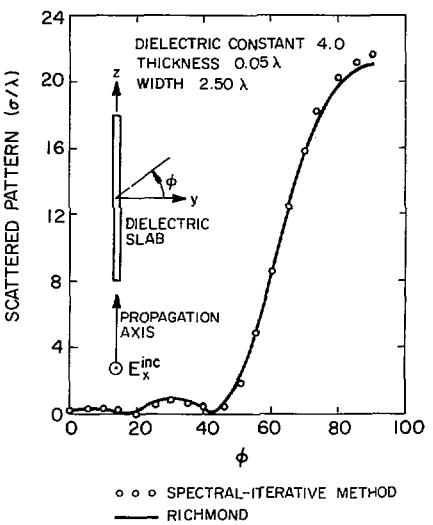

Fig. 16. Far scattered field from a dielectric strip analyzed with 11 planes.

space, i.e., both on and outside the Ewald (dispersion relationship) sphere. The SIT, in contrast, involves two-dimensional analysis using the two independent spectral variables only. This results in substantial savings both in computation time and storage requirements of SIT over the three-dimensional K-space method. A detailed quantitative comparison is given in [14] where it is shown that, compared to Bojarski's scheme, SIT is faster by a factor of 4.5, and requires storage area which is smaller by a factor of at least 9.5. Both figures are asymptotical results for large bodies.

Spectral-Iteration versus Asymptotic Techniques

Unlike asymptotic techniques, where the body must be describable as a combination of canonical structures, (which excludes, e.g., the planar corner) the SIT method does not impose restrictions on the treatable geometries apart from requiring them to conform to a rectangular grid. In addition, the built-in boundary condition check facilitates solutions of prescribed accuracy. On the other hand, the size of the scatterer cannot be increased without limit. The solution for the large example shown in Fig. 13 converged at a slower rate than for smaller cases. This suggests proximity to a region where convergence is no longer possible as was also observed by Bojarski in the three-dimensional method.

Additional Features

Two more interesting features of this method compared to matrix methods are now discussed. The first one is related to the phenomenon of instability observed in moment method solutions. One discussion [13] shows the appearance of erroneous current distributions on a rectangular cylinder around certain resonant frequencies. These currents are interpreted as belonging to waveguide modes along the hollow cylinder whose cutoff occurs at those frequencies. The appearance of these currents is caused by nature of the integral equation formulation which is confined to the surface. Homogeneous solutions to the integral equation, such as those that cause zero total field at the boundaries but a finite field within the hollow cylinder, are the cause for these erroneous results. The remedy for the situation, as suggested in [13], is the specification of additional points within the body, forcing the field to be zero throughout the body. This makes the problem well-posed and eliminates the spurious currents.

The spectral method, in contrast, requires the specification of the constitutive relationship throughout the volume anyway. Thus, it is not at all affected by internal resonance of the scatterer.

A second observation with regard to the comparison to moment methods is the simplicity with which the Green's functions are formulated in the spectral domain. The spatial representation involves Hankel functions which are not easily programmed for all ranges of the arguments, since different approximations have to be used for small and large arguments. In contrast, the spectral representation is simple and algebraic and no approximations are needed.

VII. CONCLUSION

The data-handling capability of SIT well exceeds that of the moment method. However, this advantage may not be significant for very small bodies. On the other hand, very large bodies probably cannot be handled efficiently by SIT. Consequently, it is the much needed intermediate frequency range, which is not handled very well either by MoM or the asymptotic methods, for which SIT looks most promising.

As mentioned earlier, the method presented in this paper is very conveniently extended to three-dimensional scatterers. An application of the SIT technique to a lossy dielectric cylinder of finite length will be described in a future communication [16].

The method is also expected to find additional applications to the ones that have been covered in this work (see, e.g., [15]).

REFERENCES

[1] J. B. Keller, "Geometrical theory of diffraction," *J. Opt. Soc. Am.*, vol. 28, pp. 426–444, 1957.

[2] W. D. Burnside, C. L. Yu, and R. J. Marhefka, " A technique to combine the geometrical theory of diffraction and the moment method," *IEEE Trans. Antennas Propagat.*, vol. AP-23, no. 4, pp. 551–557, July 1975.

[3] G. A. Thiele and T. H. Newhouse, "A hybrid technique for combining moment methods with the geometrical theory of diffraction," *IEEE Trans. Antennas Propagat.*, vol. AP-23, no. 1, pp. 62–69, Jan. 1975.

[4] W. L. Ko and R. Mittra, "A new approach based on a combination of integral equation and asymptotic techniques for solving electromagnetic scattering problems," *IEEE Trans. Antennas Propagat.*, vol. AP-25, no. 2, pp. 187–197, Mar. 1977.

[5] C. H. Tsao, and R. Mittra, "A spectral-iteration approach for analyzing scattering from frequency selective surfaces," *IEEE Trans. Antennas Propagat.*, vol. AP-30, pp. 303–308, Mar. 1982.

[6] R. Kastner and R. Mittra, "A spectral-iteration approach for analyzing a corrugated-surface twist polarizer for scanning reflector antennas," *IEEE Trans. Antennas Propagat.*, vol. AP-30, no. 4, pp. 673–676, July 1982.

[7] N. N. Bojarski, "K-space formulation of the electromagnetic scattering problem," *Tech Rpt* AFAL-TR-71-75, Mar. 1971.

[8] R. Kastner and R. Mittra, "A spectral-iteration technique for analyzing scattering from arbitrary bodies. Part II: conducting cylinders with H-wave excitation," *IEEE Trans. Antennas Propagat.*, pp. 535–537, this issue.

[9] R. Kastner, "Spectral-domain techniques for analyzing electromagnetic scattering from arbitrary bodies," Ph.D. dissertation, Univ. Illinois, Urbana, May 1982.

[10] K. K. Mei and J. G. Van Bladel, "Scattering by perfectly-conducting rectangular cylinders," *IEEE Trans. Antennas Propagat.*, vol. AP-11, pp. 185–192, Mar. 1963.

[11] M. G. Andreason, "Comments on "Scattering by conducting rectangular cylinders [10]," " *IEEE Trans. Antennas Propagat.*, vol. AP-12, pp. 235–236, Mar. 1964.

[12] J. H. Richmond, "Scattering by a dielectric cylinder of arbitrary cross section shape," *IEEE Trans. Antennas Propagat.*, vol. AP-13, pp. 334–341, May 1965.

[13] R. Mittra and C. A. Klein, "Stability and convergence of moment method solutions," in *Numerical and Asymptotic Techniques in Electromagnetics*, R. Mittra, Ed. New York: Springer-Verlag, 1975, ch. 5.

[14] R. Kastner and R. Mittra, "A comparative study of the stacked 2-D spectral-iterative technique, the moment method, asymptotic techniques and the Bojarski's 3-D K-Space method," presented at the Int. IEEE Antennas Propagat. Soc. Symp., Albuquerque, NM, May 24–28, 1982.

[15] ——, "Numerically rigorous inverse scattering using stacked 2-D spectral-iterative approach," presented at the Nat. Radio Sci. Meeting, Albuquerque, NM, May 24–28, 1982.

[16] ——, "A new stacked two-dimensional spectral iterative method (SIT) for analyzing microwave power desposition in biological media," to appear.

Raphael Kastner (S'80), for a photograph and biography please see page 676 of the July 1982 issue of this TRANSACTIONS.

Raj Mittra (S'54–M'57–SM'69–F'71), for a photograph and biography please see page 2 of the January 1983 issue of this TRANSACTIONS.